Binding of the Fluorescein Derivative Eosin Y to the Mitochondrial ADP/ATP Carrier: Characterization of the Adenine Nucleotide Binding Site†

Eiji Majima,‡,§ Nana Yamaguchi,‡ Hiroshi Chuman,|| Yasuo Shinohara,‡ Mayumi Ishida,‡ Satoru Goto,‡ and Hiroshi Terada*,‡

Faculty of Pharmaceutical Sciences, University of Tokushima, Shomachi-1, Tokushima 770, Japan, APRO Life Science Institute, Kurosaki, Naruto 772, Japan, and Intelligent Systems Development for Research, Kureha Chemical Industry Co. Ltd., Hyakunin-cho 3-25-1, Shinjuku-ku, Tokyo 169, Japan

Received May 7, 1997; Revised Manuscript Received November 4, 1997⊗

ABSTRACT: As the SH-reactive fluorescein derivative eosin-5-maleimide (EMA) specifically labels Cys^{159} in the second loop facing the matrix space (loop M2) of the ADP/ATP carrier in bovine heart submitochondrial particles [Majima, E., Koike, H., Hong, Y.-M., Shinohara, Y., and Terada, H. (1993) *J. Biol. Chem. 268*, 22181−22187], we studied the interaction of non-SH-reactive eosin Y, an analog of EMA, with the carrier under various conditions to characterize its binding. Eosin Y was found to inhibit ADP transport by binding to loop M2 in submitochondrial particles, but not in mitochondria. Its K_i for transport (0.33 μM) was found to be very similar to its K_d (0.53 μM) for specific binding to the carrier. Bound eosin Y was displaced by the transport substrates ADP and ATP, but not by untransportable GTP, suggesting that eosin Y bound to the specific binding site of ADP and ATP. The three-dimensional structure and electrostatic features of eosin Y were very similar to those of ADP, and the hydrophobic property and divalent charge of eosin Y were very important for its binding to the carrier. Based on these results, the features of the binding site of the transport substrates are considered.

The 30-kDa ADP/ATP carrier in the mitochondrial membrane mediates the transport of ADP and ATP across the inner mitochondrial membrane. Its functional unit is a dimeric carrier, each monomer with a six transmembrane structure (*1*−*5*). Interconversion between the two distinct conformations, the c- and m-states, of the carrier is thought to be directly associated with its transport activity: the substrate binding site in the c-state conformation faces the cytosolic side, while that in the m-state conformation faces the matrix side (*6*). The transport inhibitor carboxyatractyloside (CATR)[1] fixes the c-state conformation acting from the cytosolic side, whereas bongkrekic acid (BKA) fixes the m-state conformation acting from the matrix side. Despite extensive studies (*3*−*5*), the mechanisms of substrate recognition and transport in relation to these conformational states are not fully understood.

Chart 1: Chemical Structures of Eosin Derivatives

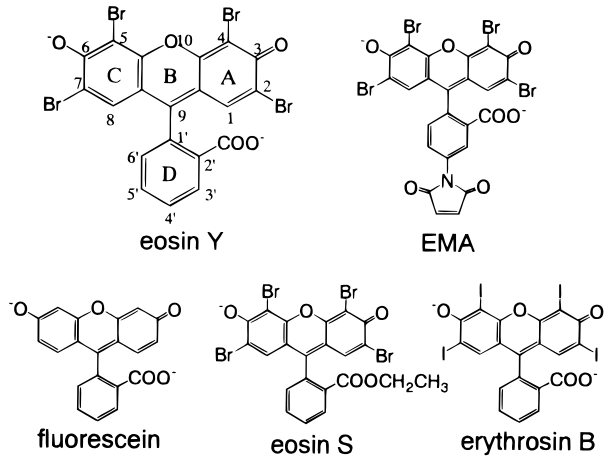

There are three loops of the ADP/ATP carrier facing the matrix space, loops M1, M2, and M3. By chemical modifications of four cysteine residues with the SH-reagents NEM and EMA, and disulfide bridge formation of cysteine residues catalyzed by copper-(*o*-phenanthroline)$_2$, we found that a pair of each of these three loops cooperatively regulates transport function of the dimeric carrier (*7*−*9*). It is noteworthy that the SH-reactive fluorescein derivative EMA very quickly and specifically labels Cys^{159} in loop M2, possibly because divalent negatively charged EMA (for chemical structure, see Chart 1) is electrostatically attracted

† This work was supported by Grants-in-aid for Scientific Research (07557164 and 08457609 to H. T.) and Scientific Research on the Priority Areas of "Channel-Transporter Correlation" (08268237 to H. T.) from the Ministry of Education, Science and Culture of Japan.

* To whom correspondence should be addressed. Fax: +81-886-33-5195. E-mail: hterada@ph.tokushima-u.ac.jp.

‡ University of Tokushima.

§ APRO Life Science Institute.

|| Kureha Chemical Industry Co. Ltd.

⊗ Abstract published in *Advance ACS Abstracts,* December 15, 1997.

[1] Abbreviations: EMA, eosin-5-maleimide; NEM, *N*-ethylmaleimide; CHAPS, 3-[(3-cholamidopropyl)dimethylammonio]-1-propanesulfonate; MES, 2-(morpholino)ethanesulfonic acid; SDS−PAGE, sodium dodecyl sulfate−polyacrylamide gel electrophoresis; BKA, bongkrekic acid; Pal-CoA, palmitoyl-CoA; CATR, carboxyatractyloside; DTT, dithiothreitol; HPLC, high-performance liquid chromatography; $R_{A,B}$, Carbo's index of similarity of the two compounds A and B; RMSD, root mean squared deviation difference; LDH, lactate dehydrogenase.

S0006-2960(97)01068-4 CCC: $15.00
Published on Web 01/06/1998

to the positively charged site(s) of loop M2, and the resulting collapse of the salt bridge(s) of this loop facilitates the labeling of Cys^{159} by the maleimide moiety of EMA. Therefore, Cys^{159} could be located at a position close to the noncovalent binding site of EMA (*7*). As this modification is counteracted by ADP, loop M2 could also constitute the primary binding site of ADP. In addition, we proposed that the cooperative swinging of these three loops is directly associated with the transport activity of the ADP/ATP carrier (*8*, *9*).

Fluorescein derivatives have been used as models of adenine nucleotides in studies of enzymes with nucleotide binding sites such as ATPases (*10*, *11*), $NAD(P)^+$-dependent dehydrogenases (*12*, *13*), and kinases (*14*, *15*), and they have also been used as probes to monitor conformational changes of enzymes such as Na^+,K^+-ATPase (*16*). Eosin Y, an analog of EMA, has the same eosin moiety consisting of a brominated xanthene ring and carboxyphenyl ring, but it cannot modify SH-residues due to lack of an SH-reactive maleimide ring (for chemical structures, see Chart 1). As EMA specifically labels Cys^{159} of the carrier, eosin Y was expected to interact specifically with the EMA binding site. If so, study of the noncovalent interaction of eosin Y with the carrier should provide useful information about the substrate binding and transport mechanism of the carrier.

We studied details of the interaction of the non-SH-reactive EMA analog eosin Y with the ADP/ATP carrier in bovine heart submitochondrial particles under various conditions. We also determined the physicochemical properties and structural features of eosin Y. Based on our results, we discuss the features of the binding site of ADP and ATP and the mechanism of their binding with the ADP/ATP carrier in relation to its transport function.

EXPERIMENTAL PROCEDURES

Reagents. EMA was purchased from Molecular Probes (Eugene). Fluorescein and eosin Y were from Wako Pure Chemical Industries (Osaka), and eosin S and erythrosin B were from Fluka (Buchs). These xanthene dyes were more than 98% pure judged by reversed-phase HPLC on an ODS column. Pal-CoA and CATR were from Sigma (St. Louis), and hydroxylapatite was from Bio-Rad (Richmond). BKA was a gift from Prof. Duine (Delft University of Technology).

Preparations of Mitochondria and Submitochondrial Particles. Mitochondria were prepared from bovine heart according to Smith (*17*) in medium consisting of 250 mM sucrose, 0.2 mM EDTA, and 10 mM Tris-HCl buffer, pH 7.2 (medium A). Submitochondrial particles containing 5 mM ATP were prepared by sonication of bovine heart mitochondria as described previously (*7*). The amounts of protein in mitochondria and submitochondrial particles were determined with a BCA protein assay kit (Pierce, Rockford) in the presence of 1% SDS using bovine serum albumin as a standard.

EMA-Labeling of the ADP/ATP Carrier. Submitochondrial particles (2 mg of protein/mL) in medium A, with or without treatment with NEM (100 nmol/mg of protein) for 10 min, were incubated with EMA at a final concentration of 20 μM at 0 °C for 30 s in the dark. The effect of eosin Y on EMA labeling was examined by preincubation of the particles with eosin Y for 10 min at 0 °C in the dark, and EMA labeling was terminated with 50 mM DTT. After pretreatment of particles with NEM, free NEM was removed by passing the samples through a column of Sephadex G-50. Then the samples were subjected to SDS−PAGE in a 12.5% polyacrylamide gel under reducing conditions by the method of Laemmli (*18*), and the fluorescence intensities of the proteins labeled with EMA were determined (*7*).

Measurement of ADP Transport. Mitochondria (2 mg of protein) and their submitochondrial particles (2 mg of protein) were suspended in medium A supplemented with 1 μg of oligomycin/mg of protein in a total volume of 1.0 mL at 0 °C. After 5 min, [^{3}H]ADP was added at a final concentration of 20 μM, ADP uptake was terminated after 10 s by addition of 5 μM CATR to mitochondria or 15 μM BKA to the particles, and ADP incorporation was determined by its radioactivity (*7*). The effect of eosin Y on ADP uptake was determined by preincubation of mitochondria or submitochondrial particles with various concentrations of eosin Y for 10 min at 0 °C in the dark. For determination of the kinetic parameters of the transport, the initial rate of ADP uptake was determined by the method of Krämer and Klingenberg (*19*).

Assay of Eosin Y Binding. The binding of eosin Y to submitochondrial particles was determined from the amounts of eosin Y released by BKA by the method of Weidemann et al. (*20*) with slight modifications. Submitochondrial particles (2 mg of protein/mL) in medium A were incubated with eosin Y for 60 min at 0 °C in the dark. The suspension was then divided into two parts, one of which was further incubated with 25 μM BKA for 30 min at 0 °C to displace eosin Y bound to the carrier. These two parts were then centrifuged at 150000 *g* for 30 min at 4 °C, the supernatants were diluted 300-fold with 100 mM Tris-HCl buffer (pH 7.2), and the amounts of eosin Y in the supernatants were determined from the fluorescence intensities at 560 nm with excitation at 530 nm. As the concentrations in the supernatants of the BKA-treated and untreated samples represent those of free plus bound eosin Y to the carrier, and free eosin Y, respectively, the amount of eosin Y bound to the carrier was determined from their difference.

The effects of various compounds on the binding of eosin Y to the carrier in submitochondrial particles were examined by incubation of the particles (2 mg of protein/mL) with 200 μM eosin Y for 60 min at 0 °C, and then with test compounds at various concentrations for 30 min at 0 °C.

Fluorescence Change of Eosin Y Bound to the Carrier. The change of fluorescence of eosin Y bound to the carrier was measured with carrier preparations solubilized with CHAPS by the method of Block and Vignais (*21*). The carrier in mitochondrial membranes solubilized with 2% CHAPS was mixed with hydroxylapatite gel (20 mg of protein/g of wet gel) equilibrated with 0.6% CHAPS, 0.1 M Na_2SO_4, and 10 mM MES buffer (pH 6.5). The supernatant obtained by centrifugation at 10000*g* for 5 min was promptly used as the carrier preparation. This preparation (5.3 μg of protein/mL) was added to eosin Y solution (final concentration, 15 nM) in medium A at 18 °C. The pH of this mixture in a total volume of 2.0 mL was 6.6. After 30 s, a test compound was added, and the fluorescence intensity of eosin Y at 560 nm with excitation at 525 nm was monitored continuously.

Determination of pK_a Values. The pK_a (pK_1 and pK_2) values of fluorescein derivatives were determined from the pH-dependent changes of the absorption spectra (*22*, *23*).

Determination of the Hydrophobic Property. The capacity factor k' on reversed-phase HPLC, as a measure of the hydrophobic property (*24*), was determined according to eq 1:

$$k' = (t_R - t_0)/t_0 \quad (1)$$

where t_R and t_0 are the retention times of test compounds and an unretained reference compound, respectively. Reversed-phase HPLC of 5 nmol of test compounds on a column of TSK gel ODS-120T (0.46 × 15 cm, Tosoh) was performed with a linear gradient (0−27% for 5 min, and then 27−72% for 50 min) of acetonitrile containing 0.05% trifluoroacetic acid at a flow rate of 1.0 mL/min. The value of log *k*' was determined from the elution times of test compounds (t_R) and that of the solvent (t_0), monitored by fluorescence intensity and absorbance at 210 nm.

Three-Dimensional Superposition. In conformational analysis, initial conformers were generated by stepwise increment of 60° with each rotatable bond, and then these structures were optimized by the AM1 semiempirical molecular orbital method. As a consequence, 2, 38, and 46 geometrically optimized low-energy minimum conformers were obtained for eosin Y, ADP, and GDP, respectively. In the three dimensional superposition, combinations of all the low-energy minimum conformers were taken into consideration. For including small conformational changes around the rotatable bonds (eq 2), the torsional variables and the energy term arising from the conformational flexibility of compounds A and B were introduced into the target function of superposition, *F*. By a combination of the extended conformational search and three-dimensional flexible superposition described here, the problem of conformational dependence on a least-squared superpositioning could be excluded (*25*):

$$F = \Sigma\omega_i|\mathbf{r}_{Ai}(\Theta_A) - \mathbf{r}_{Bi}(\Theta_B)|^2 + S[\Delta E(\Theta_A) + \Delta E(\Theta_B)] \quad (2)$$

where ω_i is the weight of *i*th atomic corresponding pair, $\mathbf{r}_i$ is the *i*th corresponding atomic position vector, Θ is the torsion angle, *S* is the scaling factor in the dimension of ($\mathbf{r}^2$/ΔE), and $\Delta E(\Theta)$ is the conformational energy. For minimizing the target function *F*, the first term in eq 2 with fixed Θ values was first minimized by the Monte Carlo method, which overcame the local minimum problems, and then minimization of the total *F* value as a function of Θ was performed. The value of $\Delta E(\Theta)$ of the second term in eq 2 was determined by molecular mechanics calculation in which only Θ was involved as an independent variable. "The goodness of superposition" of molecules A and B was evaluated by the root mean squared deviation difference (RMSD) value, determined by eq 3, of the first term in eq 2 at the minimum point of the total *F* value. On systematic search by these procedures, the best superposition of the two compounds A and B was determined:

$$\mathrm{RMSD}^2 = \sum\omega_i|\mathbf{r}_{Ai}(\Theta_A) - \mathbf{r}_{Bi}(\Theta_B)|^2/n \quad (3)$$

where *n* is the number of corresponding atomic pairs.

Comparison of Electrostatic Potentials. For comparison of the electrostatic similarities of two compounds A and B, their electrostatic potentials were evaluated by AM1. Point charges derived from the electrostatic potential of each molecule were first determined, and then their electrostatic potentials on and 4.0 Å outside the van der Waals surface of each molecule were computed from the charges. The molecular similarity between two molecules, of which superposition had already been determined, was evaluated in terms of the electrostatic potential, ρ, by the Carbo's index of similarity ($R_{A,B}$) according to eq 4 (*26*), which ranges between −1 and 1, perfect similarity being $R_{A,B} = 1$:

$$R_{A,B} = (\int \rho_A\rho_B\, d\tau)/(\int \rho_A\, d\tau \int \rho_B\, d\tau)^{1/2} \quad (4)$$

The values of ρ_A and ρ_B were calculated with each grid point at 0.3 Å intervals within the distance of 4.0 Å from the edge of the van der Waals surface of the molecule, and the space within the van der Waals surfaces was excluded from the grid points.

RESULTS

Effect of Eosin Y on Labeling of the Carrier with EMA. As halogenated fluorescein derivatives such as eosin Y, erythrosin B, and eosin S (see Chart 1), which are potent generators of singlet oxygen (*27*), could cause damage of the ADP/ATP carrier mediated by singlet oxygen, we examined the effects of 400 μM fluorescein, eosin Y, and erythrosin B on membrane proteins in bovine heart submitochondrial particles. No generation of singlet oxygen by these fluorescein dyes was observed on ESR spectrometry for at least 90 min at room temperature in the dark, whereas production of singlet oxygen was observed when the dyes were exposed to visible light (50 W) for 10 min, although not for 5 min. In addition, no change in protein bands on SDS−PAGE was observed when submitochondrial particles were incubated with 200 μM eosin Y at 0 °C for 90 min in the dark. Therefore, we concluded that fluorescein derivatives at less than 400 μM did not cause singlet oxygen-mediated damage of proteins in submitochondrial particles when the particles were incubated with dyes in the dark for at least 90 min at 0 °C. Accordingly, unless otherwise noted, the effects of fluorescein derivatives on the ADP/ATP carrier in bovine heart submitochondrial particles were examined at 0 °C in the dark within 90 min.

Bovine heart submitochondrial particles (2 mg of protein/mL) were treated with 20 μM EMA for 30 s at 0 °C in the dark. SDS−PAGE showed three fluorescent bands labeled by EMA (Figure 1A). The dominant 30-kDa fluorescent band was that of the ADP/ATP carrier, a faint 34-kDa band possibly that of the phosphate carrier (*7*), and another faint 45-kDa band that of an unidentified protein. Amino acid sequence analysis showed that Cys^{159} in loop M2 was specifically labeled by EMA under the present experimental conditions, as we reported previously (*7*). The SH-reagent NEM, which predominantly labels Cys^{56} in loop M1 but not other cysteine residues on incubation for a short period (*7*), should not have any effect on the labeling by EMA. In fact, EMA-labeling of the carrier was not affected by treatment of particles with 2 mM NEM for 10 min at 0 °C (compare Figure 1B with Figure 1A). In contrast, EMA-labelings of the 34-kDa and 45-kDa proteins were inhibited by pretreat-

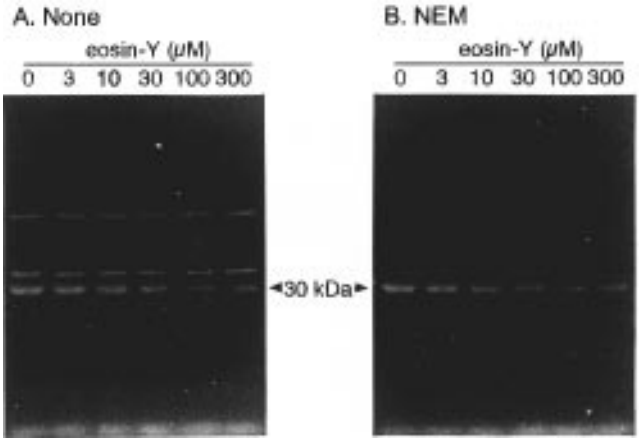

FIGURE 1: Effect of eosin Y on the labeling by EMA of membrane proteins in bovine heart submitochondrial particles without (A) and with (B) NEM pretreatment. Bovine heart submitochondrial particles (2 mg of protein/mL) were treated with various concentrations of eosin Y for 10 min, and then with 20 μM EMA for 30 s at 0 °C in medium A (pH 7.2). These treatments were carried out in the dark. After reaction with 50 mM DTT, the particles (25 μg of protein) were subjected to SDS−PAGE and fluorography. For examination of the effect of NEM (B), the particles were first treated with NEM (100 nmol/mg of protein) for 10 min at 0 °C.

Table 1: Values of 50% Inhibitory Concentrations (IC_{50}) of Various Fluorescein Derivatives for EMA-Labeling of the ADP/ATP Carrier and ADP Uptake, and Their pK_a and Capacity Factor k' Values

	IC_{50} (μM)[a]				
compound	EMA-labeling	ADP uptake	pK_1	pK_2	log k'[b]
fluorescein	>3000	600 ± 10.5	4.4	6.3	0.92
eosin Y	38.9 ± 4.2	3.33 ± 0.51	2.7	3.6	1.17
erythrosin B	17.6 ± 4.2	1.12 ± 0.47	3.8[c]		1.22
eosin S	78.3 ± 12.9	5.05 ± 0.41	−[d]	3.2	1.20

[a] Submitochondrial particles (2 mg of protein/mL) suspended in medium A in the presence of 1 μg of oligomycin/mg of protein (pH 7.2) were incubated with various concentrations of fluorescein analogs for 10 min at 0 °C in the dark. Then the suspensions were divided into two parts. One part was used for study of the effect on EMA-labeling, and the other for study of the effect on ADP uptake (cf. Experimental Procedures). [b] In three separate runs, the values of log k' were essentially the same. [c] Overlapping pK_a values. [d] Not determined due to esterification of the carboxyl group.

ment with NEM, as shown in Figure 1B, indicating that the cysteine residues in these proteins were not specifically reactive with EMA.

Next, we examined the effect of eosin Y on EMA-labeling of Cys^{159}. For this, we treated the particles with various concentrations of eosin Y for 10 min, and then with EMA for 30 s at 0 °C in the dark. As shown in Figure 1A, the fluorescence intensity of the 30-kDa band labeled by EMA decreased with increase in the concentration of eosin Y, whereas those of the 34-kDa and 45-kDa bands remained almost constant. The concentration of eosin Y for 50% inhibition of EMA-labeling (IC_{50}) was determined to be about 40 μM (Table 1). As expected, the fluorescence intensity of the 30-kDa carrier was the same with and without NEM, showing that NEM did not affect eosin Y inhibition of EMA-labeling of the carrier in the particles (Figure 1B). These results showed that eosin Y and EMA both bound to a site in loop M2 containing Cys^{159}.

Effect of Eosin Y on ADP Transport. The effect of eosin Y on ADP transport *via* the ADP/ATP carrier was studied

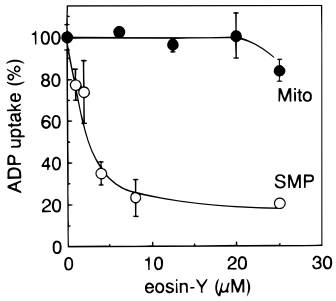

FIGURE 2: Inhibitory effect of eosin Y on ADP transport in mitochondria and submitochondrial particles. Suspensions of mitochondria (2 mg of protein/mL) and submitochondrial particles (2 mg of protein/mL) in medium A supplemented with 1 μg of oligomycin/mg of protein were treated with [^{3}H]ADP (final concentration, 20 μM) at 0 °C. After 10 s, ADP uptake was terminated with CATR and BKA, respectively. Incorporated ADP was determined from its radioactivity. The effect of eosin Y was examined by pretreatment of the mitochondria (Mito) or submitochondrial particles (SMP) with various concentrations of eosin Y for 10 min at 0 °C in the dark.

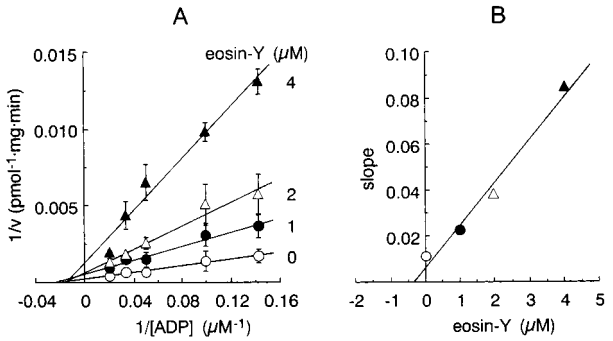

FIGURE 3: Quantitative determination of the inhibitory effect of eosin Y on ADP transport *via* the ADP/ATP carrier. The initial transport rate (v) of ADP through bovine heart submitochondrial particle membranes was determined at various concentrations of ADP ([ADP]) in the presence of fixed concentrations of eosin Y. A: Relationships between $1/v$ and 1/[ADP] at various eosin Y concentrations. B: Relationship between the slope in (A) and eosin Y concentration. The experimental conditions were as for Figure 2. All straight lines were drawn according to least-squares analyses.

by incubation of mitochondria or submitochondrial particles with eosin Y for 10 min at 0 °C. As shown in Figure 2, eosin Y at up to 20 μM did not inhibit ADP uptake by mitochondria, but at higher concentrations caused slight inhibition, its IC_{50} value being 110 μM. Eosin Y is suggested to inhibit transport activity of the ADP/ATP carrier by acting from the cytosolic side determined by the ATP-hydrolysis-related swelling of rat liver mitochondria (IC_{50}: 35 μM) (*28*). In contrast, this dye strongly inhibited ADP uptake by submitochondrial particles concentration-dependently, its IC_{50} value being about 3 μM. These results indicated that eosin Y is a potent inhibitor of adenine nucleotide transport *via* the ADP/ATP carrier by interaction with the binding site of ADP and ATP in loop M2 from the matrix side like EMA (*7*).

We measured the initial transport rate of ADP (v) in submitochondrial particles at 0 °C as a function of ADP concentration ([ADP]). From the linear relationship between $1/v$ and 1/[ADP] (Figure 3A), the K_m and V_{max} values for ADP transport were determined to be 53 μM and 4.9 nmol (mg of protein)$^{-1}$ min^{-1}, respectively, by least-squares analysis (correlation coefficient $r = 0.990$). These values

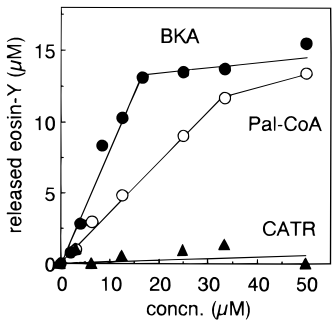

FIGURE 4: Effects of the transport inhibitors BKA, Pal-CoA, and CATR on the binding of eosin Y to submitochondrial particles. Bovine heart submitochondrial particles were incubated with 200 μM eosin Y for 1 h at 0 °C, and then with various concentrations of BKA, Pal-CoA, and CATR for 30 min in medium A. These treatments were performed in the dark. The concentration of eosin Y released was determined fluorometrically.

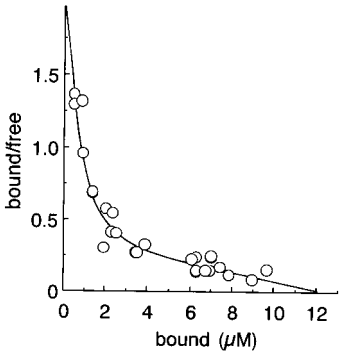

FIGURE 5: Scatchard plot of the binding of eosin Y to the ADP/ATP carrier in submitochondrial particles. Bovine heart submitochondrial particles were incubated with various concentrations of eosin Y for 1 h at 0 °C in the dark. Then bound eosin Y was released by treatment with 25 μM BKA for 30 min at 0 °C in the dark, and the total concentration (free plus bound) of eosin Y was determined. Separately, with the same particle preparation, the unbound free eosin Y concentration at the same initial eosin Y concentration was determined without BKA treatment. The concentration of bound eosin Y was determined from the difference between these values.

were similar to those reported by Lauquin et al. (*29*). Next, the inhibitory effect of eosin Y on ADP transport was examined by pretreatment of the particles with various concentrations of eosin Y for 10 min at 0 °C in the dark. The slopes of the double reciprocal plots, shown in Figure 3A, were replotted as a function of the eosin Y concentration (Figure 3B), and from the intercept on the *x*-axis of the straight line ($r = 0.989$), the K_i value of eosin Y was determined as 0.33 μM, which was about 160-fold less than the K_m value of ADP transport.

Binding of Eosin Y to the ADP/ATP Carrier. We next examined the affinity of eosin Y to the carrier relative to those of the well-known inhibitors CATR acting from the cytosolic side, BKA acting from the matrix side, and Pal-CoA acting from both sides (*30*). Submitochondrial particles were first incubated with 200 μM eosin Y for 1 h at 0 °C, and then with various concentrations of each of these inhibitors for 30 min at 0 °C. After separation of the particles, the amount of eosin Y released was determined from its fluorescence intensity in the supernatant at 560 nm with excitation at 530 nm. As shown in Figure 4, release of bound eosin Y by BKA increased linearly with increase of BKA concentration to about 15 μM and then almost leveled off, indicating that bound eosin Y was released nearly completely by BKA at 15 μM. The effect of Pal-CoA was less than that of BKA, the titer being observed at about 35 μM. CATR added to the matrix side did not have any effect at 50 μM, whereas 40 μM CATR added to the cytosolic side completely inhibited the binding of eosin Y (data not shown). These results indicated that eosin Y bound to a site common to BKA and Pal-CoA. The ineffectiveness of CATR added to the matrix side was due to its inaccessibility to the carrier, and the inhibition by CATR added to the cytosolic side was due to the induction of the c-state conformation, as observed previously (*8*, *9*).

Next, we determined the binding of eosin Y to the ADP/ATP carrier quantitatively. We determined the amount of binding of eosin Y to the carrier utilizing the fact that BKA specifically releases bound eosin Y as described above. Namely, submitochondrial particles were incubated with a known concentration of eosin Y solution at 0 °C in the dark. Then eosin Y specifically bound to the carrier was released by addition of a sufficient amount of BKA. As the nonspecific binding of eosin Y to the phospholipid membrane and proteins other than the carrier was not affected by BKA (see Experimental Procedures), the eosin Y released by BKA indicated its amount specifically bound to the carrier. A Scatchard plot of the binding of eosin Y to the ADP/ATP carrier in submitochondrial particles is shown in Figure 5. The results of this curvilinear Scatchard plot were analyzed according to the two-site model. The numbers of binding sites (maximum binding amount of eosin Y) n_1 and n_2 and the dissociation coefficients K_{d_1} and K_{d_2} were determined as $n_1 = 1.0$ nmol/mg of protein and $n_2 = 11$ nmol/mg of protein, and $K_{d_1} = 0.53$ μM and $K_{d_2} = 38$ μM. It is noteworthy that the K_{d_1} value was similar to the K_i value of ADP transport shown above, and was very close to the K_d values of adenine nucleotide analogs (*31*).

In addition, the value of n_1 was in very good agreement with the maximum amounts of BKA binding and untransportable adenine nucleotide derivatives (=1.0−1.5 nmol/mg of protein) (*8*, *31*, *32*). As these amounts correspond to the amount of the dimeric ADP/ATP carrier in bovine heart submitochondrial particles (*31*, *32*), eosin Y should bind to the dimeric carrier with 1:1 stoichiometry. Namely, the primary binding site is a pair of M2 loops of the dimerized carrier. Although the nature of the secondary binding site for eosin Y is not clear, the much higher values of n_2 and K_{d_2} than those with the primary binding site suggest that the binding of eosin Y to the secondary site is rather nonspecific.

Change in Fluorescence of Bound Eosin Y. As eosin Y is fluorophoric, its fluorescence might be changed by binding to the carrier. We solubilized the bovine heart mitochondrial ADP/ATP carrier with the mild detergent CHAPS and obtained the solubilized carrier in a fraction not adsorbed to hydroxylapatite gel. Results of SDS−PAGE of the solubilized preparation showed a very strong band of the ADP/ATP carrier, its relative amount being more than 90% judging from the intensity of its band stained with Coomassie brilliant blue, besides a few faint bands due to unidentified proteins. Of these proteins, only the carrier was labeled by EMA. The changes in the intrinsic fluorescence due to tryptophan at 345 nm with excitation at 300 nm showed that BKA readily bound to the solubilized carrier, but that ADP was necessary for the binding of CATR, indicating that the solubilized

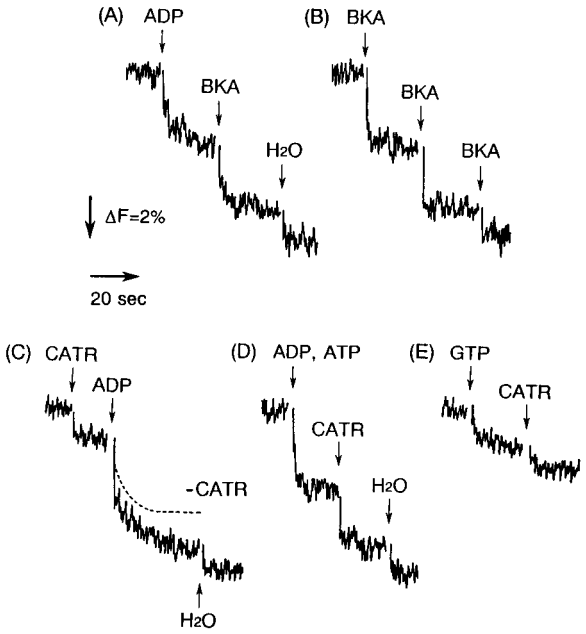

FIGURE 6: Effects of various compounds on the binding of eosin Y to the ADP/ATP carrier solubilized with CHAPS. A preparation of bovine heart mitochondria solubilized with CHAPS (5.3 μg of protein/mL) was added to 15 nM eosin Y solution at pH 6.6 and 18 °C. After 30 s, various test compounds were added in the indicated orders, and the fluorescent intensity of bound eosin Y was monitored at 560 nm with excitation at 525 nm. Change in fluorescent intensity relative to the intensity without solubilized carrier preparation is shown as ΔF. Downward deflection of the fluorescent intensity represents the release of bound eosin Y. The final concentrations of the added test compounds were 15 μM ADP, ATP, and GTP, and 150 nM BKA and CATR. The effect on the fluorescence intensity of dilution by addition of test compounds was shown by the effect of addition of the same volume (3 μL) of water.

carrier was essentially in the m-state conformation (BKA conformation) as observed by Block and Vignais (*21*). Thus, from these results, the solubilized carrier preparation was active as in the mitochondrial membrane.

As the fluorescence intensity of eosin Y added to the carrier preparation was increased, but was decreased to the same level as that of free eosin Y when the carrier was inactivated by heat-treatment at 37 °C for 1 h, decrease in the fluorescent intensity was concluded to be due to release of eosin Y from the carrier. The effects of various compounds on bound eosin Y were examined by their additions to the solubilized carrier preparation (5.3 μg of protein/mL) after its incubation with 15 nM eosin Y at 18 °C. Change in the fluorescence intensity of eosin Y was monitored continuously at 560 nm with excitation at 525 nm, at which the difference in fluorescent intensity between bound and free eosin Y was maximal.

The fluorescent intensity of eosin Y in the presence of the solubilized carrier was decreased instantly on addition of ADP (final concentration 15 μM) to about half the total change (Figure 6A). No further change was observed on addition of 150 μM ADP (data not shown), indicating that the change caused by 15 μM ADP was the maximum induced by ADP. Addition of BKA (150 nM) after ADP addition caused further decrease (Figure 6A). BKA (150 nM) in the absence of ADP decreased the fluorescent intensity considerably, and a second addition of BKA (150 nM) caused further decrease in the fluorescence to a similar level to that induced by ADP plus 150 nM BKA (compare Figure 6B with Figure 6A). In contrast, CATR at 150 nM did not cause any change in the fluorescence, and subsequent addition of ADP to a final concentration of 15 μM decreased the fluorescence greatly to the same level as that caused by ADP plus 150 nM BKA (Figure 6C). The decrease in the fluorescent intensity by CATR was observed only when ADP or ATP was present (Figure 6D). However, the untransportable nucleotide GTP, either alone or in cooperation with CATR, had no effect on the fluorescence change (Figure 6E).

As the decrease in the fluorescent intensity was associated with release of bound eosin Y, the above results suggested that the transportable nucleotides ADP and ATP displaced the bound eosin Y, and as a result the carrier was able to show transition from the m-state conformation to the c-state conformation, whereas the untransportable nucleotide GTP did not have this effect. BKA, which fixes the carrier in the m-state acting from the matrix side, released bound eosin Y without ADP. In contrast, CATR, which fixes the c-state conformation acting from the cytosolic side, could displace bound eosin Y only when the transportable nucleotides were present, because they induced the conversion of the m-state carrier to the c-state. Therefore, we conclude that eosin Y binds to the m-state carrier, and fixes this conformation.

Effects of Various Fluorescein Derivatives. To determine the structural requirements of eosin Y (tetrabromofluorescein) for binding to the ADP/ATP carrier, we examined the affinities of the fluorescein derivatives fluorescein, erythrosin B and eosin S (for chemical structures, see Chart 1) to the carrier and their effects on ADP transport. The fluorescein derivatives have a xanthene ring (A/B/C-ring) and a carboxyphenyl ring (D-ring), and divalent anionic charges are derived from a phenolic OH group in the C-ring and carboxylic acid group in the D-ring, except in eosin S, in which the carboxylic acid group is esterified. The xanthene rings of all the derivatives except fluorescein are halogenated either with four bromo groups (eosin Y and eosin S) or with four iodo groups (erythrosin B).

Like eosin Y, eosin S and erythrosin B significantly inhibited ADP transport and EMA-labeling of Cys^{159} in submitochondrial particles, but fluorescein had little effect. The IC_{50} values of ADP uptake and EMA-labeling at pH 7.2 are summarized in Table 1. The order of ADP transport inhibition was the same as that of inhibition of EMA-labeling, i.e., fluorescein << eosin S < eosin Y < erythrosin B. The results in Table 1 suggest that the halogeno groups on the xanthene ring and divalent negative charges are important for exhibition of these activities. The greater IC_{50} value of eosin Y (3.33 μM) than its K_i value (0.33 μM) for ADP transport inhibition could be due to the difference between experimental procedures: the IC_{50} was determined from the ADP uptake in 10 s, whereas the K_i was determined from the initial velocity of ADP uptake (see Experimental Procedures). Therefore, a higher concentration of eosin Y was necessary for determination of the IC_{50}.

We determined the pK_a values of the fluorescein derivatives (Table 1). As all the pK_a values of the fluorescein derivatives were less than 7, these derivatives were in anionic forms, either divalent or monovalent, under the conditions for testing their effects on ADP transport and EMA-labeling. We then determined the values of the capacity factor k' on

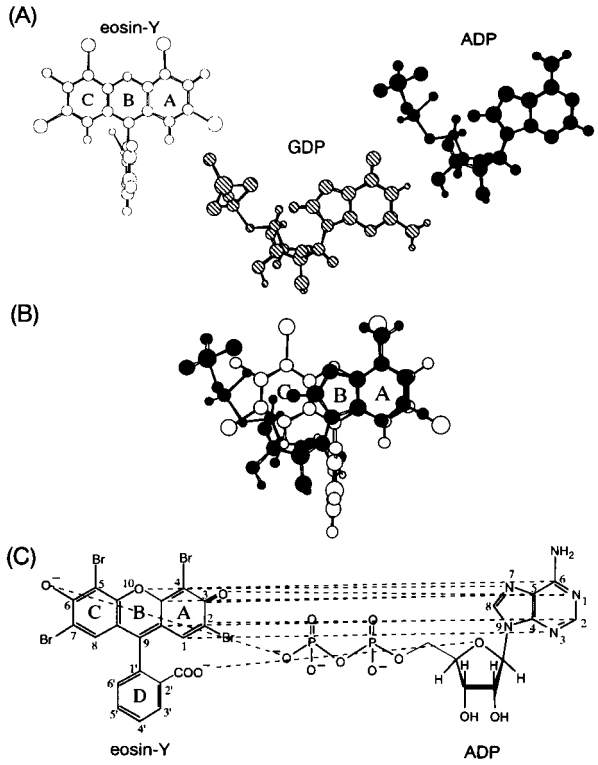

FIGURE 7: Three-dimensional structures of eosin Y, ADP, and GDP (A), superimposition of eosin Y on ADP (B), and corresponding moieties of eosin Y and ADP (C). The method for computation of superposition is described under Experimental Procedures. The ω_i value in eqs 2 and 3 was assigned as unity. In (C), corresponding atomic pairs to be superimposed are linked by discontinuous lines.

HPLC as a measure of the hydrophobic properties of compounds (*24*) according to eq 1 (see Experimental Procedures) on an ODS column at pH 2.1, in which all the test compounds had a predominantly neutral molecular form. As summarized in Table 1, log k' increased in the order fluorescein < eosin Y < eosin S < erythrosin B. The more potent inhibitory activities of erythrosin B than those of eosin Y should be due to its higher hydrophobicity. Although eosin S was more hydrophobic than eosin Y, its effects were less than those of eosin Y, possibly due to its monovalent anionic form. It is noteworthy that these activities of eosin S were still about half those of eosin Y. With the divalent fluorescein derivatives, the magnitude of ADP uptake inhibition, log ($1/IC_{50}$), increased linearly with log k' (r = 0.999), showing that the hydrophobic property is decisively important for ADP transport inhibition.

Three-Dimensional Structures and Electrostatic Potentials of Eosin Y, ADP, and GDP. The two-dimensional structure of erythrosin B has been shown to be similar to that of the *syn*-form of AMP (*33*). However, from analyses of three-dimensional structures, the *anti*-forms of adenine nucleotides are reported to be responsible for their binding to enzymes (*34*−*36*). Accordingly, we determined the most stable conformations of eosin Y, ADP, and the nontransportable nucleotide GDP by a combination of extensive conformational search and three-dimensional flexible superposition, as shown in Figure 7A. The conformation of the carboxyphenyl ring of eosin Y was perpendicular to the rigid xanthene ring to minimize its steric effect, as observed with erythrosin B (*12*, *37*). As shown in Figure 7B, eosin Y was well, but not completely, superimposed on ADP with the very small RMSD value of 0.32 Å (see eq 3). The corresponding moieties of eosin Y and ADP in the superposition are shown in Figure 7C. The energies of the conformers of eosin Y and ADP on their best superpositions were only about 0 and 3 kcal/mol, respectively, higher than those at their ground minima, showing that their superpositions were quite reasonable.

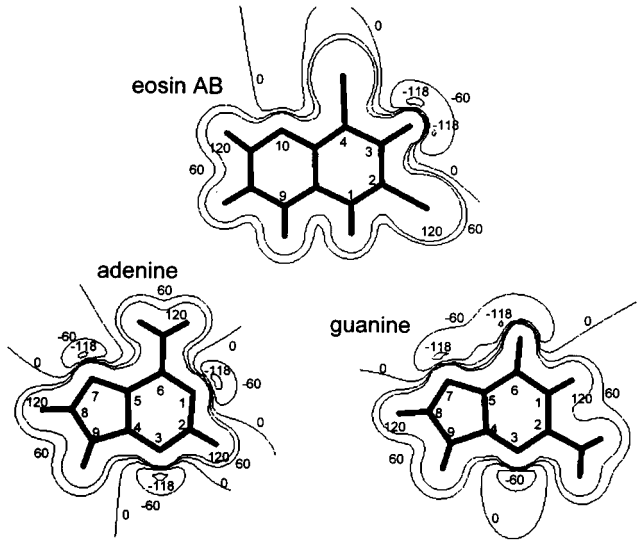

FIGURE 8: Electrostatic potential maps of adenine, guanine, and the A/B-ring of eosin Y. Electrostatic potentials were determined as described under Experimental Procedures, and electrostatic potentials are shown by contours of −118, −60, 0, 60, and 120 kcal/mol.

The A/B-ring moiety and the bonds C(9)−C(1′)−C(2′) including the carboxylate moiety of eosin Y corresponded well to the adenine moiety and the ribose ring of ADP, respectively. In addition, the phenolic OH group in the C-ring of eosin Y was located close to the β-phosphoryl group of ADP. The superposition of GDP was very similar to those of ADP and eosin Y. There was no definite difference among their stable conformations. Therefore, we next computed the electrostatic potential maps of the A/B-ring moiety of eosin Y, the adenine moiety of ADP, and the guanine moiety of GDP to determine which moieties of the A/B-ring and the adenine ring were different from that of the guanine ring. As shown in Figure 8, N(1), N(3), and N(7) of adenine; N(3), C(6)═O, and N(7) of guanine; and C(3)═O of the A/B-ring took high negative potentials, whereas other moieties took positive or null potentials. The electrostatic potential maps of adenine and guanine were essentially the same as those reported previously (*38*, *39*), and we confirmed that there was a distinct difference between the electrostatic properties of adenine and guanine (Carbo's index of similarity R = 0.35) as reported previously (*38*, *39*). In addition, we found common electrostatic features between adenine and the A/B-ring (R = 0.66): the high negative potentials of N(1) of adenine and the corresponding C(3)═O of the A/B-ring. It is noteworthy that the positive electrostatic potential at N(1) of guanine was in contrast to the negative potentials of the corresponding N(1) of adenine and C(3)═O of the A/B-ring. Therefore, the absence of a negative potential at N(1) of the guanine ring was a definite difference in its electrostatic properties from those of ADP and eosin Y. Accordingly, the negative potential of N(1) of adenine and the corresponding C(3) of eosin Y could be

of importance for specific binding to the carrier. The carrier recognizes the adenine moiety of ADP and the xanthene ring moiety of eosin Y that are distinct from the guanine moiety of GDP. These electrostatic properties should be important for molecular recognition of the substrate binding site.

DISCUSSION

In this study, we found that the non-SH-reactive fluorescein derivative eosin Y strongly inhibited ADP transport and the labeling of Cys^{159} by EMA in bovine heart submitochondrial particles but scarcely at all in mitochondria. The K_i value of eosin Y for transport (0.33 μM) was similar to the K_d value of its primary binding to the carrier (0.53 μM). These results together with the fact that EMA-labeling inhibited ADP transport (*7*) showed that eosin Y as well as EMA bound to the carrier at a position close to Cys^{159} in loop M2, causing inhibition of adenine nucleotide transport. From the inhibitory effects of ADP, ATP, BKA, and CATR on the binding of eosin Y to the carrier, eosin Y was concluded to bind to the m-state carrier from the matrix side, but not to the c-state carrier. A similar dependence of affinity on the carrier conformation was observed with 3′-[1,5-(dimethylamino)naphthoyl]adenine nucleotides (*40*). From the maximum number of eosin Y molecules bound to the primary site (n_1), eosin Y was concluded to bind to a pair of M2 loops of the dimeric carrier with 1:1 stoichiometry.

Fluorescein derivatives have been used as models of adenine nucleotides and probes to monitor conformational changes of proteins (*10*−*16*). We found that there are common structural features between eosin Y and the *anti*-form of ADP, which are responsible for binding to enzymes with a nucleotide binding site (*34*−*36*). The brominated A-ring together with the B-ring and carboxyphenyl moiety (D-ring) of eosin Y corresponds well to the adenine ring and ribose moiety, respectively, of ADP. In addition, the phenolate anionic moiety of the C-ring corresponds to the phosphate anionic moiety of ADP. In the optimized structure of eosin Y, its xanthene ring is oriented perpendicular to the carboxyphenyl ring to minimize a steric effect. This conformation is essentially the same as that of erythrosin B based on the crystallographic analysis reported by Cody (*37*). As the conformation of erythrosin B bound to LDH reported by Wassarman and Lentz (*12*) is the same as that of free erythrosin B, the eosin Y bound to the ADP/ATP carrier might take essentially the same conformation as that of the free form (see Figure 7).

As the hydrophobicity and divalent negative charges of eosin Y were found to be important for its interaction with the carrier, the hydrophobic brominated A/B-ring moiety of eosin Y should be located in the hydrophobic region of the substrate binding site of loop M2. Therefore, hydrophobic binding could be involved in the interaction of the adenine ring of ADP with its binding domain on the matrix side. In fact, the hydrophobic binding of erythrosin B has been suggested to be important in its binding to LDH (*12*). As it is suggested that for the interaction of adenine nucleotides with their related enzymes, the hydroxyl group of ribose of ADP forms a hydrogen bond with the carboxyl group of the enzymes (*41*), the hydroxyl group of ribose and the carbonyl group of the phenyl carboxylate moiety (D-ring) of eosin Y are expected to form a hydrogen bond with loop M2. In addition, N(1) of the adenine ring and the corresponding C(3)═O of eosin Y, both of which have high negative electrostatic potentials, should be responsible for hydrogen bonding with loop M2, and the β-phosphate group of ADP and the C(6) phenolate moiety of eosin Y could interact electrostatically with the phosphate binding site of the carrier.

Although the stable conformations of ADP and eosin Y are very similar to that of GDP, their electrostatic properties are different from that of GDP. Possibly, differences between the hydrogen bonding abilities of N(1) and C(6)−NH_2 of the adenine ring and those of C(2)−NH_2 and C(6)═O of the guanine ring could be a reason why GDP and GTP are not transported by the ADP/ATP carrier. Accordingly, the electrostatic interaction and/or hydrogen bonding of properly oriented ADP and ATP, and eosin Y in their binding site should be important for specific recognition and subsequent binding with loop M2. Owing to the stronger binding of eosin Y than those of transport substrates, especially due to its high hydrophobicity, eosin Y is a potent inhibitor of the transport, whereas ADP and ATP are transported owing to their weaker binding.

According to the amino acid sequence of the bovine heart mitochondrial ADP/ATP carrier (*42*), hydrophobic amino acid residues such as Phe^{153}, Leu^{156}, Ile^{160}, Ile^{163}, and Phe^{164} and charged amino acid residues and hydrogen-bond-forming amino acid residues are localized in the center portion of loop M2. As a dimer of the carrier is the functional unit, and as the paired M2 loops as well as paired M1 loops and M3 loops are suggested to be aligned symmetrically (*8*, *9*), the hydrophobic amino acid residues of M2 loops may assemble together by electrostatic interaction and hydrogen bonding, forming a hydrophobic region. These assembled segments could constitute a major binding site showing hydrophobic interaction and hydrogen bonding with eosin Y as well as EMA, and ADP and ATP in the m-state carrier. As a result, eosin Y and adenine nucleotides should bind to a dimer form of the carrier with 1:1 stoichiometry. It is noteworthy that hydrophobic amino acids and hydrogen-bond-forming amino acids are involved in the binding site of the adenine rings of various ATP and/or ADP binding proteins such as adenylate kinase and F_1-ATPase (*35*, *36*). In contrast, in view of the finding that eosin Y did not interact extensively with the carrier from the cytosolic side, the hydrophobic region of the substrate binding site may not be dominant in the c-state carrier. Therefore, gain and loss of the hydrophobic region formed by the assembled M2 loops may be associated with the interconversion of the m- and c-states of the carrier. Examination of this possibility is underway.

REFERENCES

1. Riccio, P., Aquila, H., and Klingenberg, M. (1975) *FEBS Lett. 56*, 133−138.
2. Hackenberg, H., and Klingenberg, M. (1980) *Biochemistry 19*, 548−555.
3. Walker, J. E. (1992) *Curr. Opin. Struct. Biol. 2*, 519−526.
4. Klingenberg, M. (1993) *J. Bioenerg. Biomembr. 25*, 447−457.
5. Brandolin, G., Le Saux, A., Trezeguet, V., Lauquin, G. J. M., and Vignais, P. V. (1993) *J. Bioenerg. Biomembr. 25*, 459−472.
6. Klingenberg, M. (1989) *Arch. Biochem. Biophys. 270*, 1−14.

7. Majima, E., Koike, H., Hong, Y.-M., Shinohara, Y., and Terada, H. (1993) *J. Biol. Chem. 268*, 22181−22187.
8. Majima, E., Shinohara, Y., Yamaguchi, N., Hong, Y.-M., and Terada, H. (1994) *Biochemistry 33*, 9530−9536.
9. Majima, E., Ikawa, K., Takeda, M., Hashimoto, M., Shinohara, Y., and Terada, H. (1995) *J. Biol. Chem. 270*, 29548−29554.
10. Carilli, C. T., Farley, R. A., Parlman, D. M., and Cantley, L. C (1982) *J. Biol. Chem. 257*, 5601−5606.
11. Gatto, C., and Milanick, M. A. (1993) *Am. J. Physiol. 264*, C1577-C1586.
12. Wassarman, P. M., and Lentz, P. J., Jr. (1971) *J. Mol. Biol. 60*, 509−522.
13. Brand, L., Gohlke, J. R., and Rao, D. S. (1967) *Biochemistry 6*, 3510−3518.
14. Fletterick, R. J., Bates, D. J., and Steitz, T. A. (1975) *Proc. Natl. Acad. Sci. U.S.A. 72*, 38−42.
15. Somerville, L. L., and Quiocho, F. A. (1977) *Biochim. Biophys. Acta 481*, 493−499.
16. Skou, J. C., and Esmann, M. (1983) *Biochim. Biophys. Acta 727*, 101−107.
17. Smith, A. L. (1967) *Methods Enzymol. 10*, 81−86.
18. Laemmli, U. K. (1970) *Nature 227*, 680−685.
19. Krämer, R., and Klingenberg, M. (1977) *FEBS Lett. 82*, 363−367.
20. Weidemann, M. J., Erdelt, H., and Klingenberg, M. (1970) *Eur. J. Biochem. 16*, 313−335.
21. Block, M. R., and Vignais, P. V. (1986) *Biochemistry 25*, 374−379.
22. Tamura, Z., Morioka, T., Maeda, M., and Tsuji, A. (1994) *Bunseki Kagaku* (in Japanese) *43*, 339−346.
23. Levillain, P., and Fompeydie, D. (1985) *Anal. Chem. 57*, 2561−2563.
24. Terada, H. (1986) *Quant. Struct.−Act. Relat. 5*, 81−88.
25. Chuman, H., Ito, A., Saishoji, T., and Kumazawa, S. (1995) in *Classical and Three-Dimensional QSAR in Agrochemistry* (Hansch, C., and Fujita, T., Eds.) ACS Symposium Series *606*, pp 171−185, American Chemical Society, Washington, DC.
26. Carbo, R., Leyda, L., and Arnau, M. (1980) *Int. J. Quantum Chem. 17*, 1185−1189.
27. Tomlinson, G., Cummings, M. D., and Hryshko, L. (1986) *Biochem. Cell. Biol. 64*, 515−522.
28. Beavis, A. D., Lu, Y., and Garlid, K. D. (1993) *J. Biol. Chem. 268*, 997−1004.
29. Lauquin, G. J. M., Villiers, C., Michejda, J. W., Hryniewiecka, L. V., and Vignais, P. V. (1977) *Biochim. Biophys. Acta 460*, 331−345.
30. Stubbs, M. (1981) in *Inhibitors of Mitochondrial Functions* (Erecinska, M., and Wilson, D. F., Eds.) pp 283−304, Pergamon Press, Oxford.
31. Klingenberg, M., Mayer, I., and Dahms, A. T. (1984) *Biochemistry 23*, 2442−2449.
32. Block, M. R., and Vignais, P. V. (1984) *Biochim. Biophys. Acta 767*, 369−376.
33. Neslund, G. G., Miara, J. E., Kang, J.-J., and Dahms, A. S. (1984) *Cur. Top. Cell. Regul. 24*, 447−469.
34. Kabsch, W., Mannherz, H. G., Suck, D., Pai, E. F., and Holmes, K. C. (1990) *Nature 347*, 37−44.
35. Fry, D. C., Kuby, S. A., and Mildvan, A. S. (1986) *Proc. Natl. Acad. Sci. U.S.A. 83*, 907−911.
36. Abrahams, J. P., Leslie, A. G. W., Lutter, R., and Walker, J. E. (1994) *Nature 370*, 621−628.
37. Cody, V. (1985) *Endocr. Res. 11*, 211−224.
38. Bonaccorsi, R., Pullman, A., Scrocco, E., and Tomasi, J. (1972) *Theor. Chim. Acta 24*, 51−60.
39. Giessner-Prettre, C., and Pullman, A. (1975) *Theor. Chim. Acta 37*, 335−339.
40. Klingenberg, M., Mayer, I., and Appel, M. (1985) *Biochemistry 24*, 3650−3659.
41. Wierenga, R. K., Terpstra, P., and Hol, W. G. (1986) *J. Mol. Biol. 187*, 101−107.
42. Aquila, H., Misra, D., Eulitz, M., and Klingenberg, M. (1982) *Hoppe-Seyler's Z. Physiol. Chem. 363*, 345−349.

BI9710683